Turkish Journal of Civil Engineering, 2023 27-43, Paper 739, ***Research Article***

A Relationship for Effective Thermal Conductivity of Reinforced Concrete Structures

Bekir Erdem BAS[1]
Seyednavid MARDMOMEN[2]
Guadalupe LEON[3]
Hung-Liang (Roger) CHEN[4]

ABSTRACT

Thermal conductivity is an important parameter in predicting the temperature distribution of large reinforced concrete structures. To accurately predict the temperature gradients, the effect of the steel rebar must be considered. An overall effective thermal conductivity was proposed to account for the steel reinforcement to eliminate the need to consider the complicated geometry of the rebar. In this study, the thermal conductivity of concrete cylinders embedded with 4% and 8% steel reinforcement was measured following industry standards. The effective thermal conductivity was calculated and shown to increase with the reinforcement ratio. Finite-element analysis (FEA) was conducted to model the experimental tests, and an equation was proposed to estimate the effective thermal conductivity. Additionally, FEA was used to model a concrete pier cap using the effective thermal conductivity. It was concluded that the simple effective thermal conductivity could be used to simulate the complicated steel reinforcement in concrete.

Keywords: Thermal conductivity, thermal analysis, reinforced concrete, reinforcement, finite element analysis, pier cap.

Note:
- This paper was received on May 16, 2022 and accepted for publication by the Editorial Board on April 14, 2023.
- Discussions on this paper will be accepted by September 30, 2023.
- https://doi.org/10.18400/tjce.1287651

1 General Directorate of State Hydraulic Works Technical Research and Quality Control Department, Ankara, Türkiye
erdembas@dsi.gov.tr - https://orcid.org/0000-0002-1596-0579

2 West Virginia University, Department of Civil and Environmental Engineering, Morgantown, WV, USA
semardmomen@mix.wvu.edu - https://orcid.org/0000-0001-7450-1842

3 Doane University, Department of Engineering and Physics, Crete, NE, USA
guadalupe.leon@doane.edu - https://orcid.org/0000-0002-7399-0602

4 West Virginia University, Department of Civil and Environmental Engineering, Morgantown, WV, USA
roger.chen@mail.wvu.edu - https://orcid.org/0000-0002-4278-5593

1. INTRODUCTION

A thermal analysis is a vital task needed to define the thermal stresses and cracking potential of large reinforced concrete structure. One of the most important parameters in the thermal analysis is the material's thermal conductivity. It should be defined precisely to predict the correct temperature distribution within the structure. Often, the steel reinforcement inside concrete is neglected in the thermal analysis of a reinforced concrete structure because of its layout complexity. However, steel rebars can significantly affect the overall thermal conductivity and therefore the temperature and stress distribution. Researchers have studied the effect of different mix properties (water-cement ratio, aggregate volume fraction, moisture conditions, etc.) on concrete's thermal conductivity [1-2].

There are few studies available that studied the effect of different types of inclusions (steel reinforcement, fiber, etc.) on the overall thermal conductivity of a composite. Fraternali et al. [3] investigated the thermal conductivity of recycled PET fiber reinforced concrete. Kanbur et al. [4] studied the thermal conductivity of concrete and reinforced concrete experimentally and numerically using two types of reinforcements with a diameter of 10-mm and 12-mm in three different cross-sectional geometries. Agrawal and Satapathy [5] developed a mathematical model for evaluating the thermal conductivity of polymer composites with hybrid fillers. Noh et al. [6] studied the effective thermal conductivity of reinforced concrete containing multiple layers of reinforcements. The authors developed a mathematical model to calculate the effective thermal conductivity of reinforced concrete and was validated using a finite-volume method, but their numerical simulations were not verified by experimental test. Kim et al. [7] studied the thermal conductivity of lightweight aggregate concrete with a high volume of entrained air using a heat flow meter. Yun et al. [8] evaluated the thermal conductivity of lightweight concrete materials with various lightweight aggregate and glass bubbles using a linear and plane heat source methods. To efficiently predict the temperature gradients in a reinforced concrete structure, a simplified effective thermal conductivity model to consider the effect of steel reinforcement inside concrete is needed.

In this study, the CRD-C 36-73 method [9] was used to measure the thermal conductivity of mortar samples with and without steel reinforcement. Then, the experimental results were compared to a 3-D thermal analysis calculation using ABAQUS finite element analysis (FEA) software. Finally, the FEA software was used to simulate reinforced concrete with various volumetric reinforcement ratios and an empirical equation was developed to calculate the effective thermal conductivity. The effective thermal conductivity was used to predict the temperature time history of a reinforced concrete bridge pier cap at the center and side locations.

2. EXPERIMENT

Six 15-cm (6-in) diameter by 30.5-cm (12-in) height cylinder specimens were prepared. Three specimen layouts were prepared: plain mortar, plain mortar plus six steel rebars, and plain mortar plus eleven steel rebars. Each layout had two-cylinder specimens. The steel rebars were all 46-cm (18-in) long and 1.27-cm (0.5-in) in diameter. The mortar mix design is shown in Table 1. The mortar mix was selected to provide more uniform samples in the cylinders since coarse aggregates may segregate due to the steel rebar spacing. The locations of the steel rebars are shown in Figure 1.

Table 1 - Mix design

Material	Weight Density (kg/m^3)
Cement	521.8
Sand	1513.2
Water	256.8

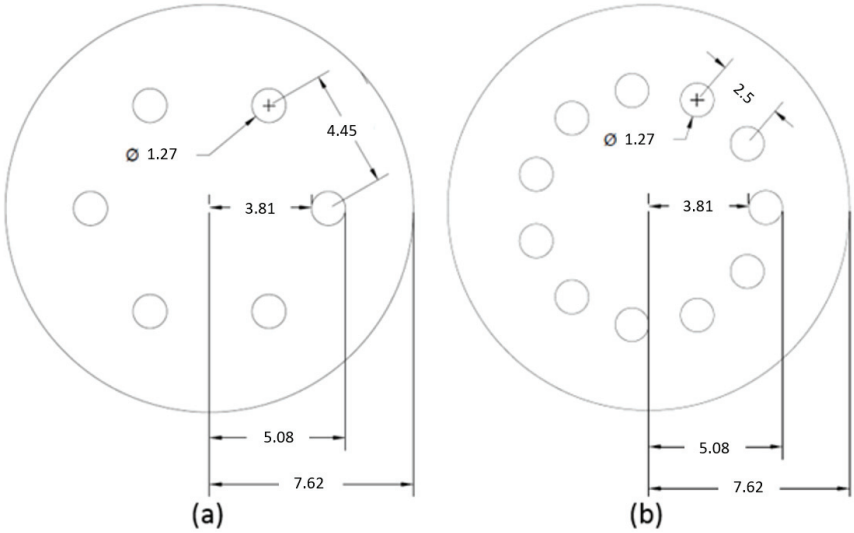

Figure 1 - Specimens' layout of (a) Mortar + 6 steel rebars (b) Mortar + 11 steel rebars (Dimensions are in cm)

Three K-type thermocouples were inserted in each cylinder. They were located at the center, 4.5-cm (1.75-in) from the center and 7-cm (2.75-in) from the center. All the thermocouples were in the middle of the cylinders and fixed with multiple zip ties. The locations of the thermocouples are shown in Figure 2. In order to maintain the location and the spacing of the rebars, two pieces of plywood with holes at the locations of the steel rebar were placed on the top and the bottom of the plastic mold. The specimens were cured for 14-days with a curing temperature of 43 °C which is more than 28-days of curing at a reference temperature of 23 °C. After the curing process was completed, each specimen was placed in a hot water bath with a heating unit to reach 75 °C. Then, each specimen was placed on top of two pieces of plywood and submerged in a cold-water bath. The temperature of the water was kept constant throughout each experiment by circulating the water. The temperature of the water was measured using a thermocouple placed 5-cm from the side of the specimen. The mortar and water temperatures were recorded at an interval of 5-seconds until the concrete's surface temperature reached the water temperature. Each test was repeated two times. The reinforced specimens are shown in Figure 3.

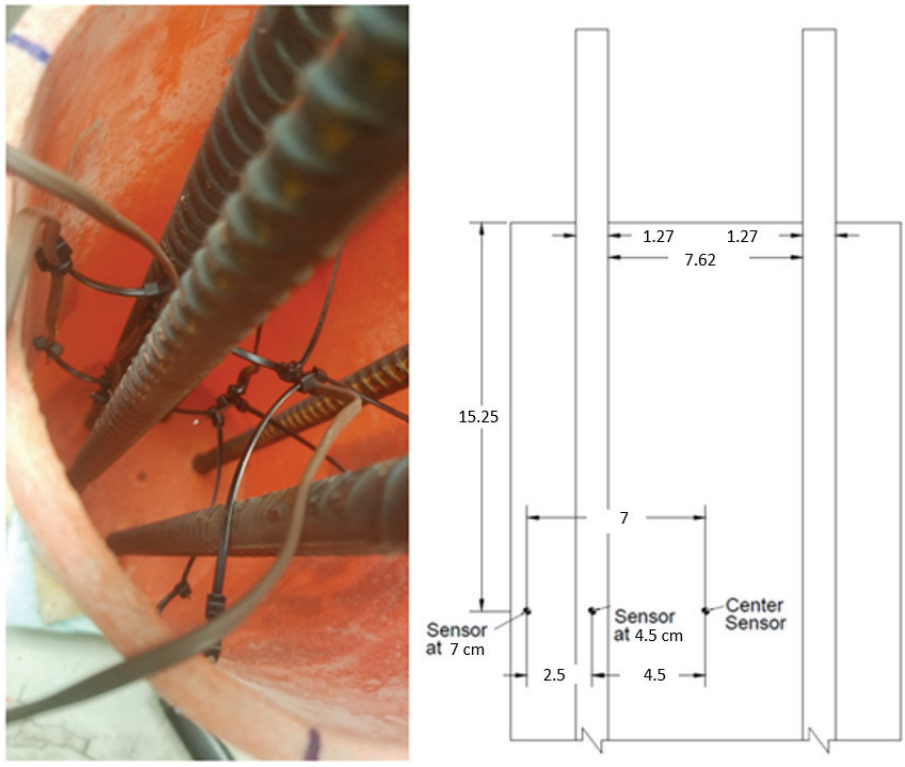

Figure 2 - Location of Thermocouples (Dimensions are in cm)

(a) (b)

Figure 3 - Reinforced specimens (a) Mortar + 6 steel rebars (b) Mortar + 11 steel rebars

3. ANALYSIS OF RESULTS

The overall thermal conductivity can be calculated using the equations provided by CRD-C 36-73:

$$\alpha = \frac{K}{\rho C_p} = \frac{M}{(t_2 - t_1)} \quad , \qquad M = \frac{60\ Ln\left(\frac{T_1}{T_2}\right)}{\left(\frac{5.783}{r^2} + \frac{\pi^2}{l^2}\right)} \tag{1}$$

where α is the thermal diffusivity (m^2/h), M (m^2) is a factor depending on the size and shape of the specimen, t_1 and t_2 are the times at which the center of the specimen reaches the specified temperature differences (min), T_1 and T_2 are the temperature differences between the specimen and water bath (°C) at times t_1 and t_2, r is the radius of the cylinder (m), l is the length of the cylinder (m), K is the thermal conductivity ($W/m/K$), ρ is the weight density (kg/m^3), and C_p is the specific heat capacity ($J/kg/K$). Based on the dimensions of the cylinder and assuming T_1 and T_2 are 33.33 °C and 11.11 °C, M can be calculated to be 0.0598 (m^2). The specific heat of mortar can be calculated using Equation 2 [10], [11].

$$C_{p-mortar} = \frac{(740\rho_{cem} + 710\rho_s + 4184\rho_w)}{\rho_{mortar}} \tag{2}$$

where ρ_{cem}, ρ_s, ρ_w are the weight densities (kg/m^3) of the cement, sand, and water in the mortar mix design. $\rho_{mortar} = \rho_{cem} + \rho_s + \rho_w$. The effective thermal conductivities were obtained and are shown in Table 2. As shown in Table 2, the effective thermal conductivities of the cylinders with steel reinforcement increased by 16.9% and 22.3%.

Finite element analysis (FEA) software (ABAQUS) was used to simulate the thermal behavior of the cylinders. For the cylinders with the steel rebar, the reinforcements were bonded with the mortar using a tie constraint (i.e. perfect bond). The three-dimensional thermal transient analysis was performed using hexahedral linear elements (DC3D8). An element size of 1.5-mm (0.06-in) was used for the mortar and steel rebar. An example of the geometry and mesh for a concrete cylinder with 11 steel rebars is shown in Figure 4. A total of 989,400 and 149,600 elements were used in this model for concrete and steel rebars, respectively.

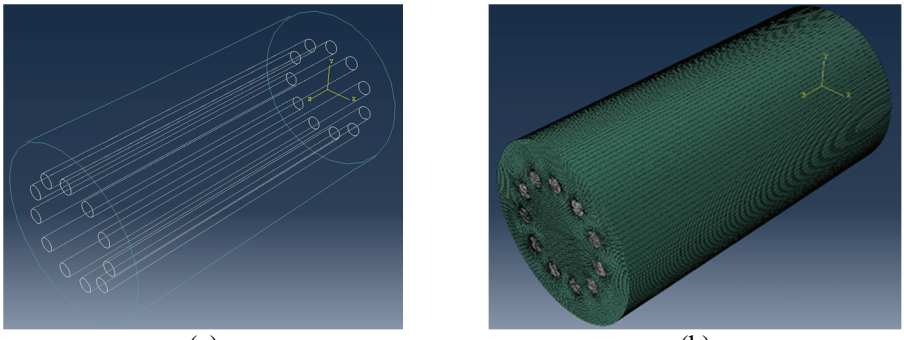

(a) (b)

Figure 4 - (a) 3-D Geometry and (b) mesh of the thermal analysis model with 11 steel rebars

The FEA temperature distribution at the middle of the cylinder at 10 minutes is shown in Figure 5. The temperature-time histories were exported and compared with the experimental results in Figure 6. The convection boundary condition had a film coefficient (convection coefficient) of 4500 W/m^2/K and was assumed to model the effect of the circulating water. The temperature of the cold-water bath stayed close to 13 °C in all the experiments. As shown in Figure 6, the FEA results compare well with the experimental temperatures measured at different locations. The largest variation occurs with the sensors closest to the surface. The measured initial concrete temperature and the water temperature were used as an input for each case. Since the experimental initial temperatures of the 4.5-cm and 7-cm thermocouples are not the same as the center temperature, due to a delay of about 1-minute between taking the cylinders out of the hot water bath and submerging it in the cold-water bath, the FEA initial temperature input at different locations was adjusted accordingly.

Table 2 - Specific heat and thermal conductivity

Material	Mass Density (kg/m^3)	Specific Heat (J/kg/K)	Thermal Conductivity (W/m/K)
Steel	7897.1	502.4	53
Mortar	2291.8	1106	2.253
Mortar + 6 steel rebars	2529.7	1026	2.633
Mortar + 11 steel rebars	2727.9	970	2.755

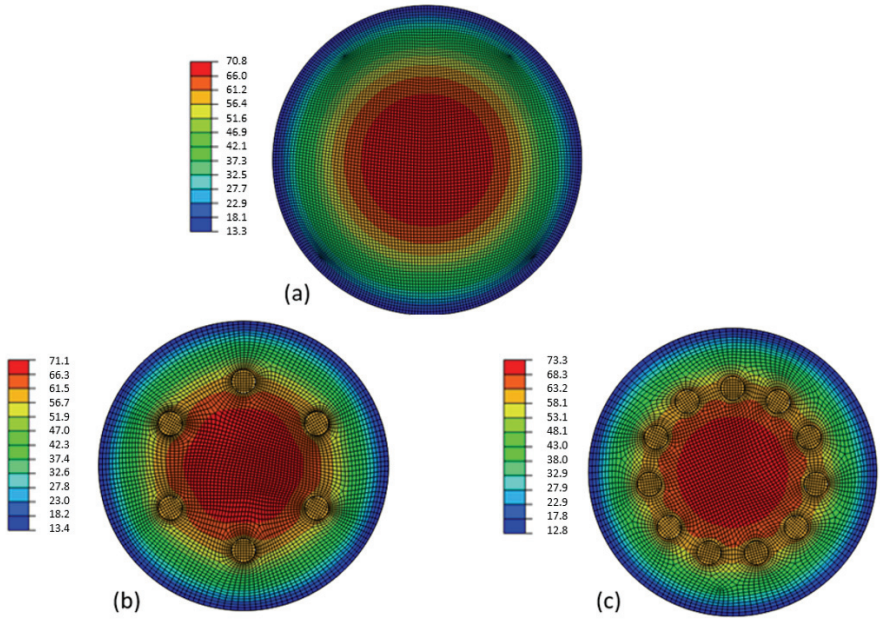

Figure 5 - Temperature distribution at 10 min for (a) mortar (b) mortar + 6 steel rebars (c) mortar + 11 steel rebars (temperatures are in °C) at the middle of the cylinder

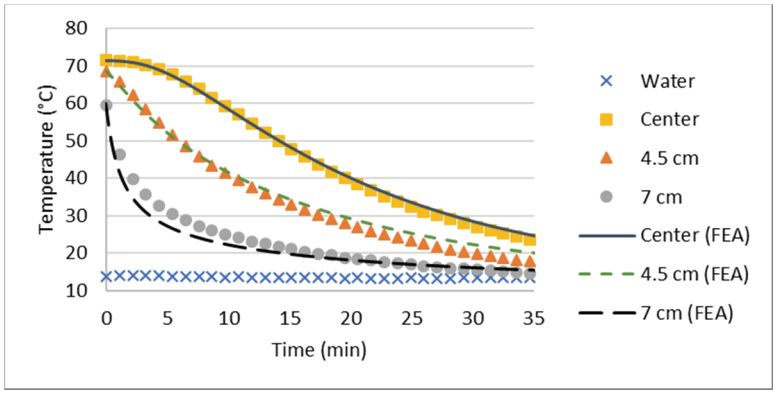

(a)

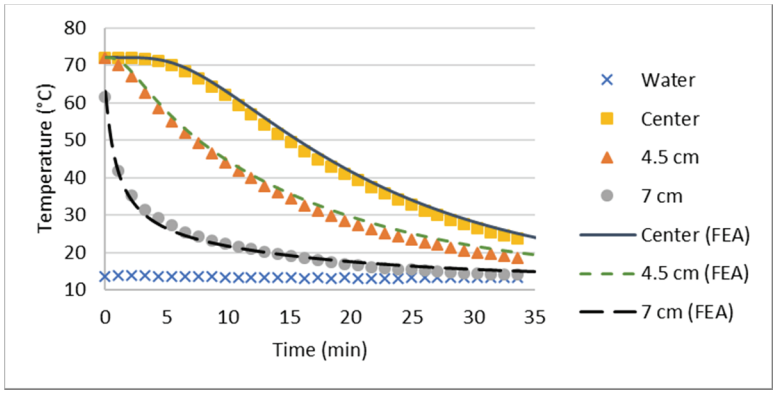

(b)

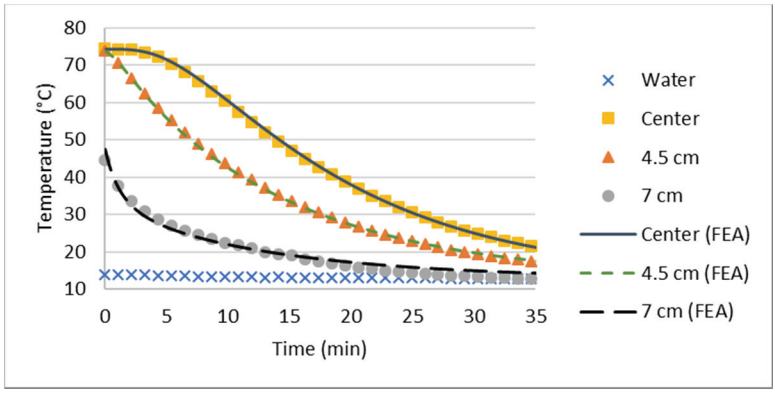

(c)

Figure 6 - Temperature time history comparisons of experiment and FEA at different locations: (a) plain mortar (b) mortar + 6 steel rebars (c) mortar + 11 steel rebars

4. EFFECTIVE THERMAL CONDUCTIVITY

Another set of 3-D FEA models was used to develop an effective thermal conductivity equation. The effective thermal conductivity could be used to estimate the thermal conductivity of concrete with complicated steel reinforcement [12]. In these analyses, the temperature-time history of the cylinders with different reinforcement ratios was calculated using the material properties mentioned in Table 2. The temperature decays were obtained for cylinders with 3, 5, 7, 9 and 11 steel rebars using the same clear cover spacing (1-inch (2.54 cm) from the surface of the cylinder) for all the analyses. An initial concrete temperature of 100 °C and a constant water temperature of 20 °C were chosen to calculate the effective thermal conductivities. The time period it took for the temperature difference between the center location of the cylinder and the water temperature to reach from 44.44 °C to 11.11 °C was used to calculate the effective thermal conductivities. An M of 0.0755 (m^2) was calculated based on the mentioned temperature differences and the dimension of the cylinder using Equation 1. The linear relationships of the natural logarithm of the temperature difference versus time (shown in Figure 7 (a)) from FEA calculations indicate

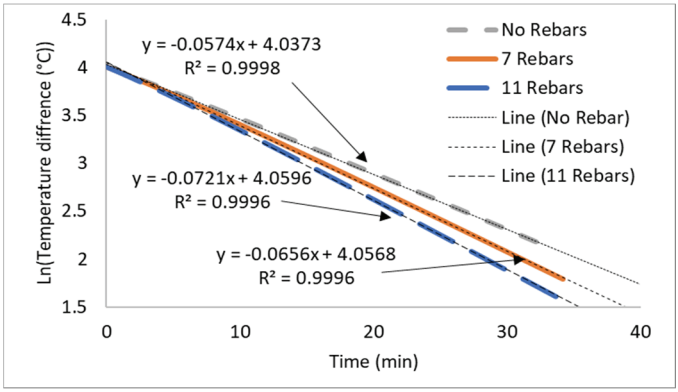

(a)

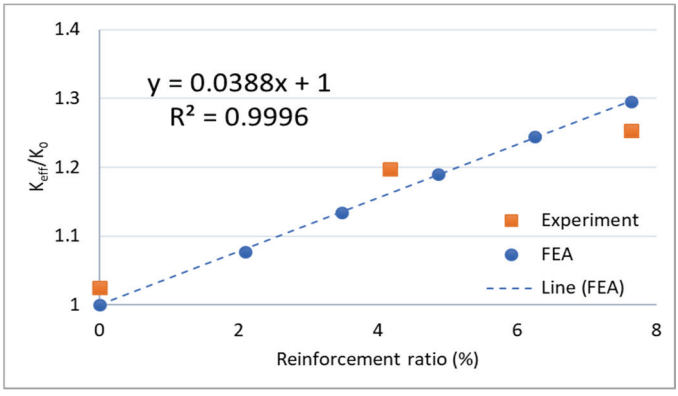

(b)

Figure 7 - (a) Natural logarithm of temperature difference vs. time, (b) Normalized effective thermal conductivity vs. volumetric reinforcement ratio

that the homogeneous solution in Equation 1 can still be a reasonable estimation in the calculation of the effective thermal conductivity of concrete with rebar. Using the FEA results, the normalized effective thermal conductivity (K_{eff}/K_0) versus the percentage of reinforcements (by volume) can be calculated, and the results are shown in Figure 7 (b). The fitted trendline is shown in Equation 3. The value of K_0 was obtained to be 2.198 $\mathrm{W/m/K}$ based on the temperature decay calculated by the FEA calculation, which is about 2.5% difference with the measured value of 2.253 $\mathrm{W/m/K}$. Using the proposed Equation 3, the effective thermal conductivities of the mortar with 6 steel rebars (4.24% reinforcement ratio) and 11 steel rebars (7.78% reinforcement ratio) are 2.546 and 2.846 $\mathrm{W/m/K}$. The calculated values are 3.4% and 3.2% different than the experimental values calculated using Equation 1 as shown in Table 2. A comparison of the calculated thermal conductivities and the measured data is displayed in Figure 7 (b).

It is noted that for a typical reinforced concrete structure, the reinforcement amount in different direction can be different. However, to simplify the calculation, the concrete structure will be assumed to have same K_{eff} along all directions when using Equation 3. Typically, for a mass concrete structure, the heat conduction along one critical direction (smallest dimension direction) will be the highest and can be assumed almost insulated from the other two directions. Therefore, the simplified K_{eff} can be used to estimate the critical temperature gradient with enough accuracy, which will be more efficient than using a complicate reinforcement geometry. An example of this application will be shown in Section 5.

$$\frac{K_{eff}}{K_0} = 0.0388\ (reinforcemnt\ ratio\ (\%)) + 1 \qquad (3)$$

5. THERMAL ANALYSIS OF A PIER CAP

The relationship provided in Equation 3 was used to analyze an Ices Ferry bridge's pier cap constructed in Cheat Lake, West Virginia (shown in Figure 8). FEA software using ABAQUS with a user subroutine described previously by Lin and Chen [10] was used to perform the thermal analysis. The details of the thermal analysis parameters and the mix design properties for the concrete pier cap are shown in Table 3 where h_{cv} ($\mathrm{W/m^2/K}$) is the convection coefficient between the steel formwork's surface and the ambient environment and h_c ($\mathrm{W/m^2/K}$) is the conductance coefficient between the steel formwork's surface and the concrete's surface.

In the thermal analysis, the heat generation rate, $q(t)$ of each concrete element was calculated using Equation 4. In Equation 4, t_e is the equivalent age of concrete which is calculated based on Equation 5 to consider the time shift due to the temperature dependency of chemical reactions between the cementitious materials and water. In addition, the specific heat of concrete, C_{p-con}, and thermal conductivity of concrete, K_c, were considered to be degree of hydration dependent parameters [13], [14] and shown in Equation 6 and Equation 7.

$$q(t) = H_u W_{cem} \alpha_u \, exp\left(-\left[\frac{\tau}{t_e}\right]^{\beta}\right)\left[\frac{\tau}{t_e}\right]^{\beta}\frac{\beta}{t_e} exp\left(-\frac{E_a}{R}\left(\frac{1}{T(t)+273}-\frac{1}{23+273}\right)\right) \quad (4)$$

$$t_e = \int_0^t \exp\left(-\frac{E_a}{R}\left(\frac{1}{T(t)+273}-\frac{1}{23+273}\right)\right) dt \quad (5)$$

$$C_{p-con}\big(\alpha_r, T(t)\big) = \frac{1}{\rho_c}(W_{cem}\alpha_r(8.4T(t)+339) + (740P_{cem} + 720P_{FA})W_{cem}(1-\alpha_r) + 710W_s + 840W_a + 4184W_w) \quad (6)$$

$$K_c(\alpha_r) = K_{uc}(1.33 - 0.33\big(\alpha_r(t)\big) \quad (7)$$

where H_u (J/kg) is the ultimate heat of hydration, W_{cem}, W_s, W_a, W_w are the masses of the cementitious materials, sand, coarse aggregate and water per unit volume of concrete (kg/m^3), t_e is the equivalent age of concrete, α_u, τ, β are the hydration parameters, *t* is the time, *T(t)* is the temperature of concrete (°C), R is the universal gas constant (8.314 J/mol/K), E_a is the activation energy of concrete (J/mol), $\alpha_r(\mathrm{t}) = \alpha'(\mathrm{t})/\alpha_u$, $\alpha'(\mathrm{t})$ is the degree of hydration of the concrete. ρ_c is weight density of concrete $(\mathrm{kg/m^3})$; $\rho_c = W_{cem} + W_s + W_a + W_w$, and P_{cem}, P_{FA} are the mass fractions of cement and fly ash in the cementitious materials. K_{uc} is the thermal conductivity (W/m/K) of the mature concrete (measured after 28 days of curing).

The adiabatic temperature rise of the mix was measured using an adiabatic calorimeter developed from a previous study [10]. The heat loss was minimized by controlling the surrounding water temperature and matching its temperature with the concrete sample. The measured adiabatic temperature rise was fitted to find the hydration parameters shown in Table 3. The ultimate heat of hydration (H_u) was calculated using the cement chemical compositions and fly ash amount in the mix [15]. The ultimate degree of hydration was calculated using an equation based on the water cementitious ratio and the percentage of fly ash [16]. A comparison between the measured and fitted adiabatic temperature rise is shown in Figure 9. The parameter shown in Table 3 was used to calculate the heat generation rate of the concrete, Equation 4, and the heat generation function is shown in Figure 10. The Ices Ferry pier cap geometry is shown in Figure 11(a). By using the concrete parameters in Table 3, the temperature distributions in the pier cap were calculated using ABAQUS, and a typical temperature distribution plot at 20 hours is shown in Figure 11(b).

Table 3 - Mix design and hydration parameters.

Mix Design (kg/m^3)					**Thermal Analysis Parameters**						
Cement	Fly ash	Water	Coarse Agg.	Fine Agg.	α_u	H_u	τ	β	E_a	h_{cv}	h_c
334.6	44.4	142	1,032	736	0.69	425,520	7.8	0.95	44,000	11.4	358

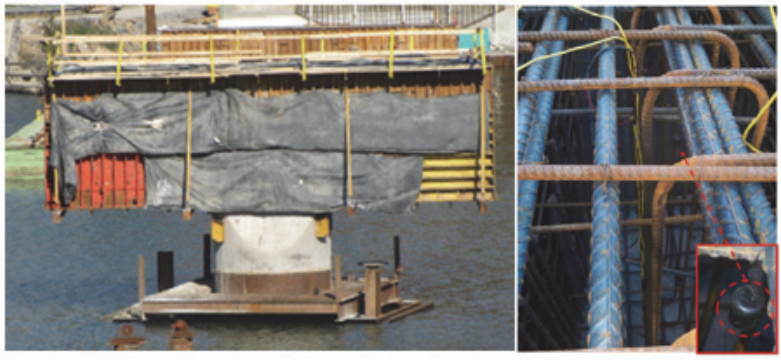

(a)

(b)

Figure 8 - (a) Ices Ferry Bridge pier cap (b) Pier cap's rebar cage

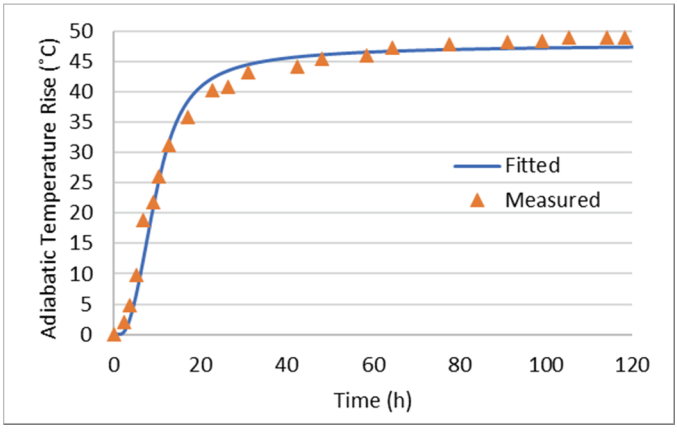

Figure 9 - Adiabatic temperature rise

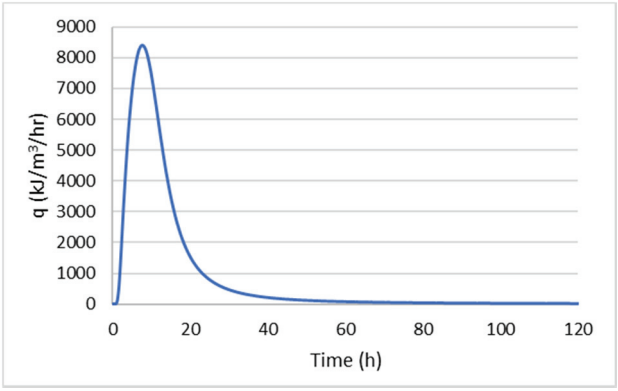

Figure 10 - Input heat generation function

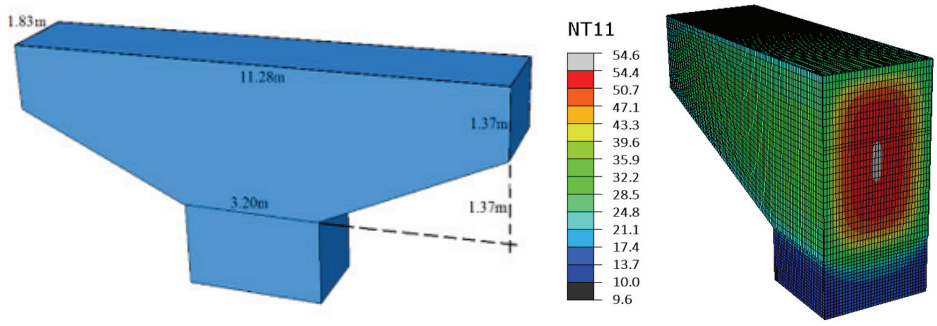

(a) (b)

Figure 11 - FEA analysis of Ices Ferry Bridge pier cap (a) Dimensions (b) Temperature distribution in °C at 20 hours (cut at the center)

The pier cap structure was heavily reinforced (Figure 8). Therefore, the effect of the reinforcement needs to be considered in the thermal analysis. The plain concrete thermal conductivity was measured to be 2.1 W/m/K. The effect of different reinforcement ratios on the temperature of the pier cap at the cap center and at the side surface (5 cm away from the front side) are shown in Figure 12 and Figure 13. As shown in these figures, due to a higher reinforcement ratio, a higher temperature decay could be seen on the calculated center temperature after reaching the peak temperature (at around 20 hours) than the temperature decay at the side location. The effect of different reinforcement ratios on the temperature at the side surface is not as severe as at the center. The effective thermal conductivity with an assumed 8% reinforcement ratio was calculated as 2.75 W/m/K using Equation 3. These thermal conductivity values were used as K_{uc} in the thermal analysis calculations. Therefore, the following equation can be replaced by Equation 7:

$$K_c(\alpha_r) = K_{uc}\big(0.0388\,(reinforcemnt\ ratio\ (\%)) + 1\big)\big(1.33 - 0.33\big(\alpha_r(t)\big)\big) \qquad (8)$$

The temperature-time histories calculated using the FEA at the center of the pier cap and 5 cm away from the front side of the pier cap were compared to the experimental data. The comparison is shown in Figure 14. Results show that when using the plain concrete thermal conductivity, the concrete temperature (orange line) at the center of the pier cap would be overestimated. The temperature predictions improved by considering the steel reinforcement with the calculated effective thermal conductivity (black dashed line) as shown in Figure 14. It can be seen that by considering the effective thermal conductivity, the temperature differential (difference between the center temperature and the side temperature) in the pier cap is also reduced which indicates a reduction of the thermal stress at the side surface. However, further study considering the actual reinforcement cage is recommended in order to have a better estimation of the effect on the thermal stress of the pier cap.

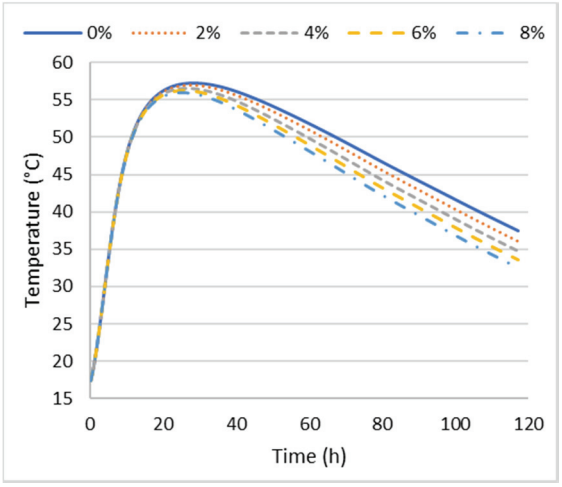

Figure 12 - Effect of reinforcement ratio on center temperature

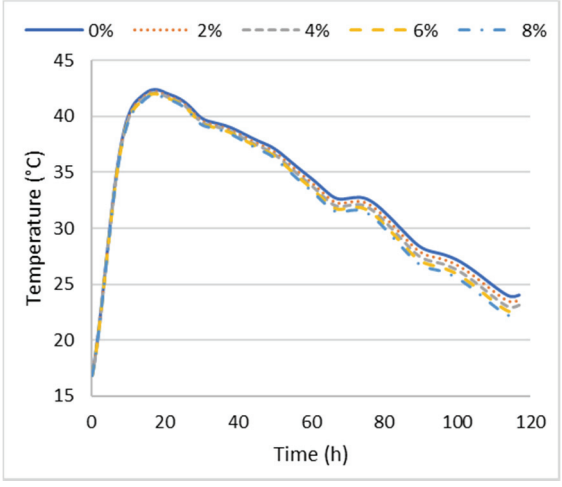

Figure 13 - Effect of reinforcement ratio on front side surface temperature

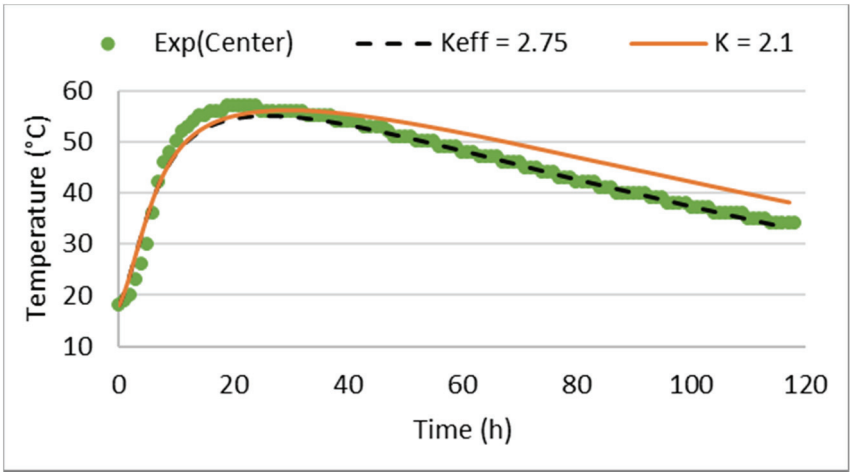

(a)

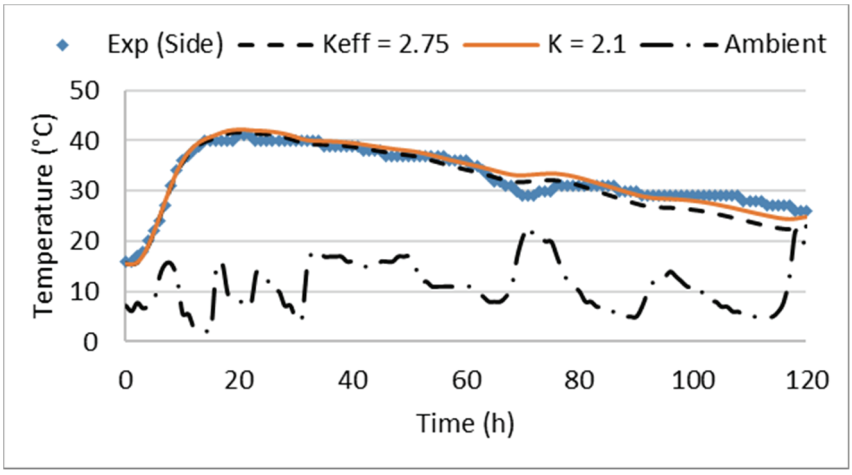

(b)

Figure 14 - Concrete temperature time history of the Ices Ferry Bridge pier cap at (a) Center of the pier cap and (b) 5cm from the front side surface (Thermal conductivity, K $(W/m/K)$)

6. CONCLUSIONS

In this study, the thermal conductivity of mortar cylinders with 15-cm (6-in) diameter embedded with 6 and 11 steel rebars with 1.27-cm (0.5-in) diameter was experimentally measured. CRD-C 36-73 was used to calculate the thermal conductivities based on the temperature decay of the center. Besides the center temperature, two other locations, 4.5 cm and 7 cm from the center were monitored. FEA was conducted and successfully predicted the experimental measurements. The experimental measurements showed a thermal

conductivity increase of 16.9% and 22.3% by embedding 6 and 11 steel rebars in the cylinders. Then, the FEA was used to develop a linear effective thermal conductivity equation that can be used in the thermal analysis of reinforced concrete elements without complicated rebar modeling. Finally, the proposed equation was used in a finite element temperature analysis of a real bridge pier cap to evaluate the accuracy of the prediction. Results show that the temperature predictions improved at the center location by considering the steel reinforcement with the calculated effective thermal conductivity.

Symbols

C_p	:	Specific heat capacity $(\mathrm{J/kg/K})$
$C_{p-mortar}$	:	Specific heat capacity of mortar $(\mathrm{J/kg/K})$
C_{p-con}	:	Specific heat capacity of concrete $(\mathrm{J/kg/K})$
E_a	:	Activation energy of concrete (J/mol)
H_u	:	Ultimate heat of hydration (J/kg)
K	:	Thermal conductivity $(\mathrm{W/m/K})$
K_c	:	Time dependent thermal conductivity of concrete (W/m/K)
K_{uc}	:	Thermal conductivity of mature concrete (W/m/K)
K_0	:	Thermal conductivity of non-reinforced concrete (W/m/K)
K_{eff}	:	Effective thermal conductivity (W/m/K)
l	:	Length of the cylinder (m)
r	:	Radius of the cylinder (m)
R	:	Universal gas constant (8.314 J/mol/K)
t	:	Time (h)
T	:	Temperature of concrete (°C)
t_1, t_2	:	Times at which the center of the specimen reaches the specified temperature
T_1, T_2	:	Temperature differences between the specimen and water bath (°C)
t_e	:	Equivalent age of concrete (h)
W_{cem}, W_s W_a, W_w	:	Mass of the cementitious materials, sand, coarse aggregate, and water per unit volume of concrete (kg/m^3)
α	:	Thermal diffusivity (m^2/h)
α'	:	Degree of hydration of the concrete
α_r	:	Degree of reaction of concrete

α_u, τ, β	:	Hydration parameters
ρ_{mortar}	:	Weight density of mortar (kg/m^3)
$\rho_{cem}, \rho_s, \rho_w$	:	Weight densities of the cement, sand, and water in the mortar mix (kg/m^3)

Acknowledgments

The authors acknowledge the support provided by the West Virginia Transportation Division of Highways (WVDOH) and FHWA for Research Project WVDOH RP#312. Special thanks are extended to our project monitors, Mike Mance, Ryan Arnold and Donald Williams of WVDOH. The authors also appreciate the assistance from Yun Lin, Alper Yikici, the District 4 engineers and the construction crew for the Ices Ferry bridge project.

References

[1] Kim, K.-H., Jeon, S.-E., Kim, J.-K., and Yang, S., "An experimental study on thermal conductivity of concrete," *Cement and Concrete Research*, vol. 33, no. 3, pp. 363–371, Mar. 2003, doi: 10.1016/S0008-8846(02)00965-1.

[2] Davraz, M., Koru, M. and Akdağ, A.E.,"The Effect of Physical Properties on Thermal Conductivity of Lightweight Aggregate," *Procedia Earth and Planetary Science*, vol. 15, pp. 85–92, Jan. 2015, doi: 10.1016/j.proeps.2015.08.022.

[3] Fraternali, F., Ciancia, V., Chechile, R., Rizzano, G., Feo, L., and Incarnato, L.,"Experimental study of the thermo-mechanical properties of recycled PET fiber-reinforced concrete," *Composite Structures*, vol. 93, no. 9, pp. 2368–2374, Aug. 2011, doi: 10.1016/j.compstruct.2011.03.025.

[4] Kanbur, B., Atayilmaz, S., Demir, H., Koca, A., and Gemici, Z., "Investigating the Thermal Conductivity of Different Concrete and Reinforced Concrete Models with Numerical and Experimental Methods," *Advances in Mechanical Engineering Applications*, 2013.

[5] Agrawal, A. and Satapathy, A., "Mathematical model for evaluating effective thermal conductivity of polymer composites with hybrid fillers," *International Journal of Thermal Sciences*, vol. 89, pp. 203–209, Mar. 2015, doi: 10.1016/j.ijthermalsci.2014.11.006.

[6] Noh, H.G., Kang, H.C., Kim, M.H., and Park, H.S., "Estimation Model for Effective Thermal Conductivity of Reinforced Concrete Containing Multiple Round Rebars," *International Journal of Concrete Structures and Materials*, vol. 12, no. 1, p. 65, Oct. 2018, doi: 10.1186/s40069-018-0291-2.

[7] Kim, H.K., Jeon, J.H., and Lee, H.K., "Workability, and mechanical, acoustic and thermal properties of lightweight aggregate concrete with a high volume of entrained air," *Construction and Building Materials*, vol. 29, pp. 193–200, Apr. 2012, doi: 10.1016/j.conbuildmat.2011.08.067.

[8] Yun, T.S., Jeong, Y.J., Han, T.S., and Youm, K.S., "Evaluation of thermal conductivity for thermally insulated concretes," *Energy and Buildings*, vol. 61, pp. 125–132, Jun. 2013, doi: 10.1016/j.enbuild.2013.01.043.

[9] US Army Corps of Engineers, "CRD-C36-73 Method of Test for Thermal Diffusivity of Concrete," CRD-C36-73, 1973.

[10] Lin, Y. and Chen, H.-L., "Thermal analysis and adiabatic calorimetry for early-age concrete members," *Journal of Thermal Analysis and Calorimetry*, vol. 122, no. 2, pp. 937–945, Nov. 2015, doi: 10.1007/s10973-015-4843-2.

[11] Van Breugel, K., "Prediction of temperature development in hardening concrete," *Prevention of thermal cracking in concrete at early ages*, vol. 15, pp. 51–75, 1998.

[12] Bas, B. E., "Study on The Thermal Properties of Concrete Containing Ground Granulated Blast Furnace Slag, Fly Ash and Steel Reinforcement," M.S. Thesis, West Virginia University, 2020.

[13] Kyle, J., Riding, A., Schindler, A., Juenger, M., and Folliard, K., "Evaluation of Temperature Prediction Methods for Mass Concrete Members," *ACI Materials Journal*, vol. 103, no. 5, Sep. 2006, doi: 10.14359/18158.

[14] Van Breugel, K., "Artificial cooling of hardening concrete." Report, Delft University of Technology, 1980.

[15] Chen, H.-L., Mardmomen, S., and Leon, G., "On-site measurement of heat of hydration of delivered mass concrete," *Construction and Building Materials*, p. 121246, Oct. 2020, doi: 10.1016/j.conbuildmat.2020.121246.

[16] Schindler, A. K. and Folliard, K. J., "Heat of Hydration Models for Cementitious Materials," *Materials Journal*, vol. 102, no. 1, Jan. 2005, doi: 10.14359/14246.